



BRNO UNIVERSITY OF TECHNOLOGY

VYSOKÉ UČENÍ TECHNICKÉ V BRNĚ

FACULTY OF MECHANICAL ENGINEERING

FAKULTA STROJNÍHO INŽENÝRSTVÍ

ENERGY INSTITUTE

ENERGETICKÝ ÚSTAV

EXCESSIVE PRESSURE ENERGY RECOVERY IN LIQUID TRANSPORT SYSTEMS

REKUPERACE PŘEBYTEČNÉ TLAKOVÉ ENERGIE PŘI TRANSPORTU KAPALIN

BACHELOR'S THESIS

BAKALÁŘSKÁ PRÁCE

AUTHOR

AUTOR PRÁCE

Samuel Luky

SUPERVISOR

VEDOUCÍ PRÁCE

doc. Ing. Pavel Rudolf, Ph.D.

BRNO 2024

Assignment Bachelor's Thesis

Institut: Energy Institute
Student: **Samuel Luky**
Degree program: Fundamentals of Mechanical Engineering
Branch: Fundamentals of Mechanical Engineering
Supervisor: **doc. Ing. Pavel Rudolf, Ph.D.**
Academic year: 2023/24

As provided for by the Act No. 111/98 Coll. on higher education institutions and the BUT Study and Examination Regulations, the director of the Institute hereby assigns the following topic of Bachelor's Thesis:

Excessive pressure energy recovery in liquid transport systems

Recommended bibliography:

MELICHAR, J.; BLÁHA, J. a VOJTEK, J. Malé vodní turbíny. Vydavatelství ČVUT, 1998.

BEDNÁŘ, J. Malé vodní elektrárny 2. Turbíny. SNTL, 1989.

SOUZA, D.E.S.; MESQUITA, A.L.A a BLANCO, C.J.C. Pump-as-turbine for energy recovery in municipal water supply networks. A review. Journal of the Brazilian Society of Mechanical Sciences and Engineering. 2021.

NEIPP, A. a RIEDELBAUCH, S. Numerical Investigation of Blade Lean and Sweep affecting Secondary Flows in an Axial Expansion Turbine. IOP Conf. Series: Earth and Environmental Science. 2016, roč. 49.

Deadline for submission Bachelor's Thesis is given by the Schedule of the Academic year 2023/24

In Brno,

L. S.

doc. Ing. Jiří Pospíšil, Ph.D.
Director of the Institute

doc. Ing. Jiří Hlinka, Ph.D.
FME dean

Abstrakt

Táto práca sa zaoberá využitím prebytočnej tlakovej energie vo vodovodných potrubíach a spôsobmi ako ňou produkovať elektrinu. V prvej časti sú zhrnuté všetky použiteľné riešenia, to sú čerpadlová turbína, AXENT a STRAFLO turbína a turbína s protibežnými obežnými kolesami. Druhá časť je venovaná návrhu axiálnej turbíny pre špecifickú samosprávu mesta Ferlach v Rakúsku. Návrh je následne otestovaný pomocou zjednodušeného CFD výpočtu pomocou programu ANSYS fluent. Výsledky sú zhodnotené a ďalšie kroky na zlepšenie sú navrhnuté.

Klíčová slova

obnova energie, PRV, turbína, CFD

Summary

This thesis deals with unutilised pressure in liquid transport pipelines and possibilities to convert them to electricity. The first part evaluates all the current solutions, that is Pump as turbine, AXENT or STRAFLO turbine and counter rotating turbine and summarizes their advantages and disadvantages. The second part of the work is dedicated to designing an axial turbine to a specific municipality of Ferlach in Austria. This turbine design is afterwards evaluated through a simplified CFD simulation using ANSYS fluent. The results are assessed and further design improvements are proposed.

Keywords

energy recovery, PRV, turbine, CFD

BIBLIOGRAPHIC CITATION

LUKY, Samuel. *EXCESSIVE PRESSURE ENERGY RECOVERY IN LIQUID TRANSPORT SYSTEMS* [online] [cit. 2024-05-24].. Brno, 2024. Bakalářská práce. Vysoké učení technické v Brně, Fakulta strojního inženýrství. doc. Ing. Pavel Rudolf, Ph.D.

STATEMENT OF THE THESIS ORIGINALITY

I honestly declare that this thesis "Excessive pressure energy recovery in liquid transport systems" was written only by me under the leadership of my supervisor and with the use of sources listed in the Bibliography

Samuel Luky

ACKNOWLEDGEMENTS

I would like thank doc. Ing. Pavel Rudolf, Ph.D. for his guidance throughout the creation of this thesis, he always gladly answered to all the questions that i presented.

Samuel Luky

Contents

Introduction	9
2 Theoretical introduction	10
2.1 Energy	10
2.2 Velocity triangles	10
2.3 Euler turbine equation	11
3 Current solutions	12
3.1 Pump as Turbine (PAT)	12
3.2 In-line axial turbine	14
3.3 Counter rotating runners	16
3.4 Spherical lift turbine	19
4 Turbine design	21
4.1 Basic parameters	21
4.2 Approach to turbine design	21
4.3 Angles β_1 and β_2 1	22
4.4 Camber line	23
4.5 Blade thickness	24
4.6 Giving thickness to the camber line	25
5 CFD simulation	26
5.1 Creating geometry using CAD	26
5.2 Creating the mesh	26
5.3 Fluent setup	28
5.4 Postprocessing	29
5.5 Conclusion after the first iteration	30
5.6 Second iteration	31
5.7 Counter rotating turbine	34
Conclusion	37
Literature	38
NOMENCLATURE	40

Introduction

The consequences of climate change are forcing the entire world to move away from fossil fuels towards cleaner renewable energy. Although hydro power is by far the biggest source of renewable energy right now predictions suggest slower growth rate compared to other renewables seen in Figure 1. This can be explained by a few reasons, in developed countries the most optimal hydro power sites are already utilized, lower investments compared to other renewables and droughts caused by climate change[1].

In Europe natural reaction is a big push towards making Mini (less than 1 MW) and Micro (less than 100 kW) hydro power potential more economically viable[2].

Excess pressure energy in Water distribution networks and pipes in the process industry is quite a common problem. In water distribution networks its caused by a big elevation differences where the energy is not used up and in the process industry where the pressure is a byproduct of various industry processes. This is often resolved by installing a Pressure reduction valve which transfers the pressure into heat and thus wasting the energy. By installing a turbine the pressure is reduced to a safe value and electricity is generated. In some remote areas where connection of the grid isn't possible the energy can be used to power sensors that gather data.

Harnessing this free energy is one of the steps towards emission free future. This bachelor thesis looks at all known possible technical solutions and compares them to each other.

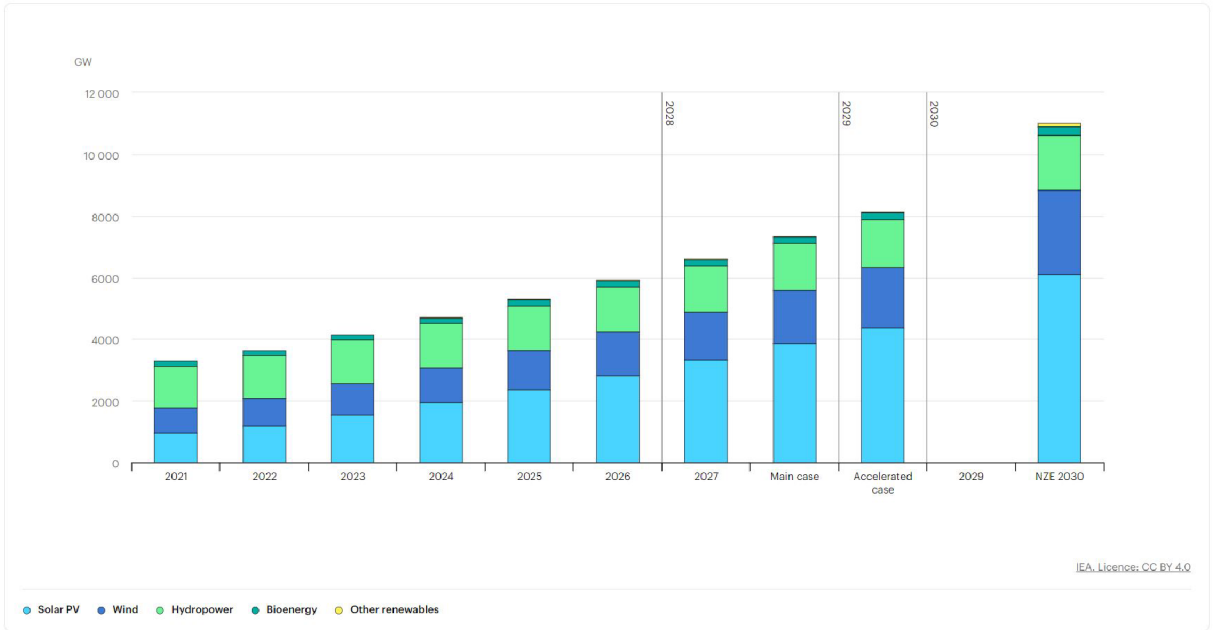


Figure 1: Future energy production predictions [1]

2 Theoretical introduction

2.1 Energy

Specific energy is defined as energy per unit mass [J/kg].

Total specific energy in a stable flow can be defined as a sum of individual energies.

$$E = E_z + E_k + E_p \quad (2.1)$$

where: $E_z = gh$, $E_k = \frac{1}{2}v^2$, $E_p = \frac{p}{\rho}$

By using the law of conservation of energy at the inlet and outlet we get the theoretical energy available.

$$E_1 - E_2 = g(h_1 - h_2) + \frac{1}{2}(v_1^2 - v_2^2) + \frac{1}{\rho}(p_1 - p_2) \quad (2.2)$$

In this thesis, only flow in horizontal water pipelines will be examined where $h_1 = h_2$ can be written, the equation then simplifies.

$$E_1 - E_2 = \frac{1}{2}(v_1^2 - v_2^2) + \frac{1}{\rho}(p_1 - p_2) = \Delta E \quad (2.3)$$

Power can be defined as.

$$P = \rho Q \Delta E \quad (2.4)$$

These equations are valid only for ideal, in-viscid and in-compressible fluids.

Efficiency is defined as.

$$\eta = \frac{P_t}{P_{flow}} \quad (2.5)$$

Efficiency is used to evaluate the quality of water turbine energy transformation. The understanding of these basic equations will be fundamental for understanding the later chapters.

2.2 Velocity triangles

For visualisation and description of the flow velocity triangles are used, this can be seen in Figure 2. Individual velocities go by \vec{c} , \vec{u} , \vec{w} , for absolute velocity, tangential velocity and relative velocity respectively. Indexes 1 and 2 represent the velocity at the leading and trailing edge respectively. Absolute velocity is the sum of all individual velocities and represents the velocity of water in relation to a static object like turbine case and can be expressed by the following equation.

$$\vec{c} = \vec{u} + \vec{w} \quad (2.6)$$

Tangential velocity represents the velocity of some point at some distance from the said runner. and relative velocity represents the velocity of the flow as if the runner is not moving. Absolute velocity is made out of 2 components, meridian absolute velocity \vec{c}_m which is always perpendicular to tangential velocity and circumferential component of absolute velocity \vec{c}_u oriented in tangential direction representing the circulation of the fluid. Angle α represents the angle made by β and \vec{u} , in typical turbine solutions represents the angle of guide vanes. β is the angle between \vec{w} and \vec{u} , typically called the angle of the blade.

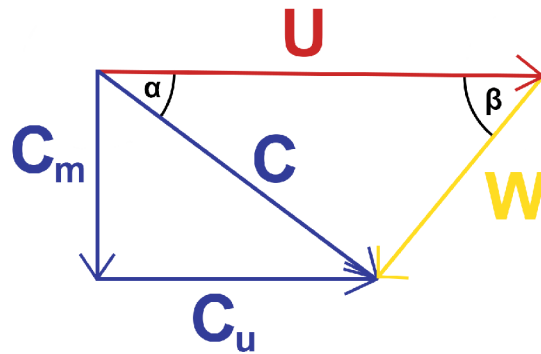


Figure 2: Velocity triangles

2.3 Euler turbine equation

The fundamental equation for turbo-machinery application is the **Euler energy equation for turbomachinery**. It is generally valid for all rotating channels.

$$E\eta = u_1c_{u1} - u_2c_{u2} \quad (2.7)$$

The circumferential velocities are basically constant and all that can be influenced are the absolute velocity components in the circumferential direction.



Figure 3: Installation site of PAT [3]

3 Current solutions

3.1 Pump as Turbine (PAT)

Pump as turbine (PAT) refers to a practice of using a pump to generate electricity opposed to its primary function of moving fluid or creating pressure. In this mode the direction of flow is reversed and power is not consumed but generated[2] This approach is particularly common in small-scale or micro hydro power, where flow rates and heads are relatively low[2].

Probably the biggest reason to use PAT is the economic viability, economy of scale dwarfs the price down compared to traditional turbines (Francis, Kaplan) that are manufactured to a specific location, simultaneously shortening the return of investment. The Euler equation is still applicable, the efficiency in turbine mode is different but not necessarily lower[2]. The efficiency remains quite high although for different operating conditions. Another advantage of PAT is they most likely come with a food safety certificate, that is important since it will come with direct contact with drinking water[5]. One of the problems with using PAT is the unknown Best efficiency point (BEP)of the machine in turbine mode. Generally the manufacturers only test the pumps in pump mode and their hydraulic characteristic curves are quite different in turbine mode. Another problem is regulation of PAT, the flow rate and pressure head in Water distribution networks are not constant, with variable conditions BEP is not sufficient and complete hydraulic characteristic curve is needed[6]. Today there are methods for their prediction based on Computational fluid dynamics (CFD) but they require complete model dimensions of the pumps that aren't widely available plus they are always only predictions with an error, even up to 30% [6]. With using a pump in reverse mode a few challenges are encountered, the axial load is reversed and this means the bearing are being operated in conditions not designed for[7]. The leading edge is the trailing edge in PAT operation, this decreases

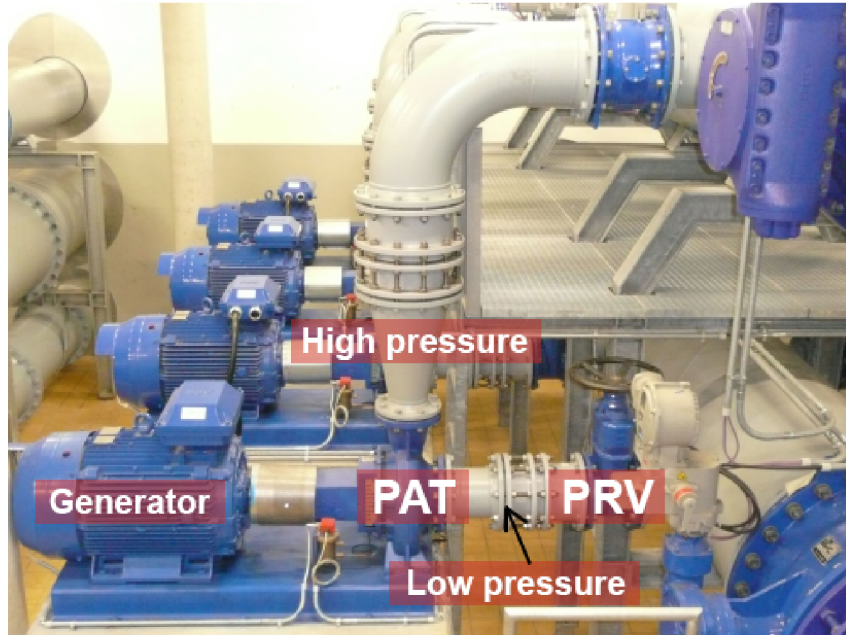


Figure 4: KSB Etanorm pumps operating as turbines in a water pumping station; adjusted according to[4]

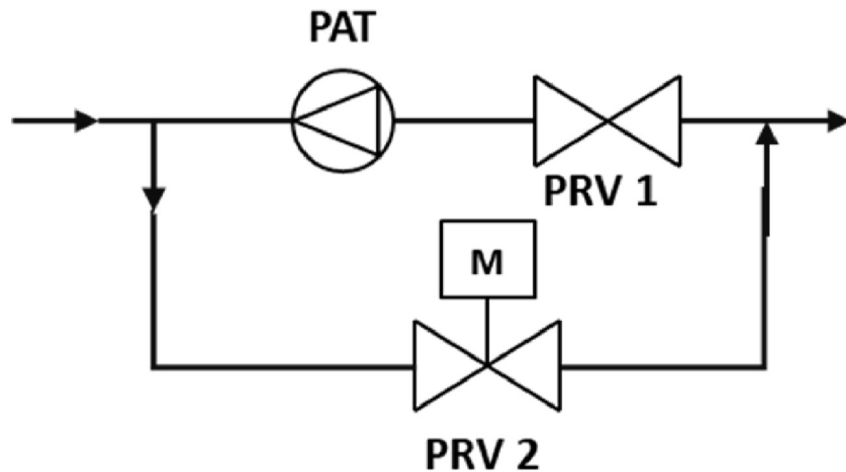


Figure 5: Scheme of hydraulic regulation[6]

efficiency.

This brings the need for regulation which there are quite a few options, traditional hydro power plants operate multiple machines at partial load capacity so they can divide the available flow based on each machines BEP, but for micro hydro (there is only one machine available) there is either hydraulic or electric regulation[6]. Hydraulic regulation is done with installing two PRVs, one in series and one in parallel, this can be seen in Figure 5, the first PRV in series absorbing the overpressure, the second PRV in parallel absorbing the overflow[6]. By this configuration we can achieve fixed velocity at BEP in PAT even under variable conditions[5]. Electric regulation is done with frequency inverters, placed in between the grid and generator, which can regulate the velocity of the runner based on upstream conditions [6]. Both methods have been tested and results were inconclusive, for electric regulation you can only control the runner velocity for some specific number of values, most probably far away from BEP, for hydraulic regulation there are always

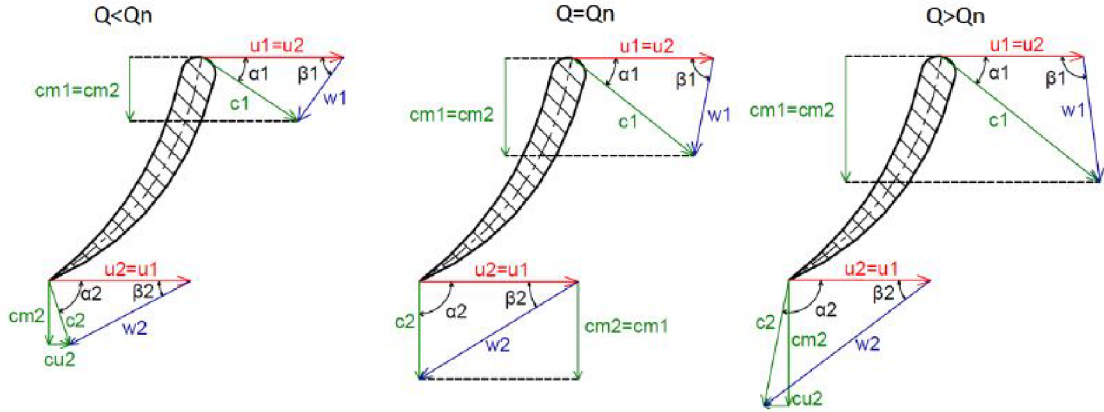


Figure 6: Velocity triangles under variable conditions where Q_n is the optimal flow rate [8]

losses from the function of PRV[6]. By combining these two methods, higher efficiencies were achieved but the draw back being higher investments cost[6]. Another disadvantage is the installation of PAT, due to the technical layout of pumps, they cannot be installed in-line, this increases the civil works costs and in most suitable locations there is already little room for this, we can see this in Figure 3.

Most common use of PAT is in the process industry, this includes waste water treatment plants, paper factories but also water pumping stations seen in Figure 4 places where there is already a need of a pump.

3.2 In-line axial turbine

In-line axial turbines are favourable in energy harvesting mainly for their simplicity and cost-effectiveness. The big reason for their use in energy harvesting is possibility of in-line installation which saves costs and space. The turbine can consist in multiple variations, the most simple variant is just single runner with no stator blades, stator blades can be added also with additional blade pitch adjustment mechanism. Mechanical regulation of blade pitch angle is quite a complex and expensive addition, this makes it inappropriate to PRV harvesting application. This type of turbine is more suitable for large flow rates and smaller heads, this can to some point be solved by adjusting the number of blades and their chord length [2]. Since all the blades are fixed only the velocity of the runners can be regulated with frequency inverters. Velocity triangles can be seen in Figure 6.

There are two suitable construction variants that have been tested for application in water network pipelines. The one where the water flows around the generator and one where it flows through the generator. **Commercially called AXENT and STRAFLO respectively.**

The first AXENT style turbine where the water flows around the generator was invented by Escher Wyss company in 1936 [2]. The AXENT turbine is a modular two stage axial turbine which depending on the situation can have one or two stages and it is optimized to be capable of utilizing higher heads than regular axial turbines [9]. The generator sits inside a hydrodynamically optimized bulb in front or back of the turbine and

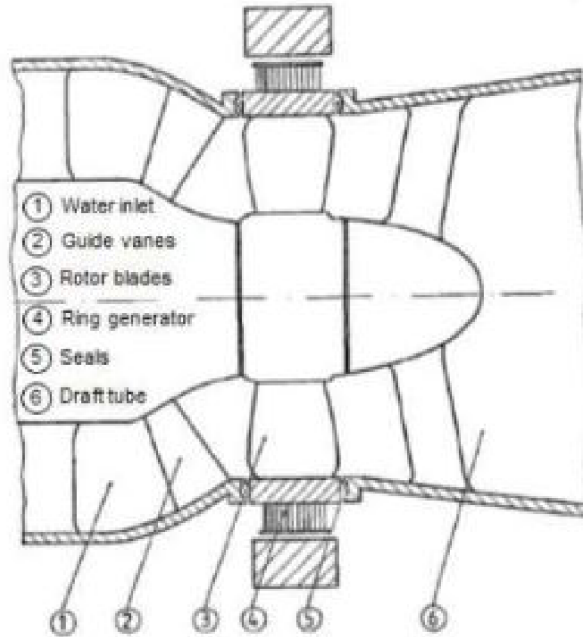


Figure 8: Cross-section of a STRAFLO turbine[12]

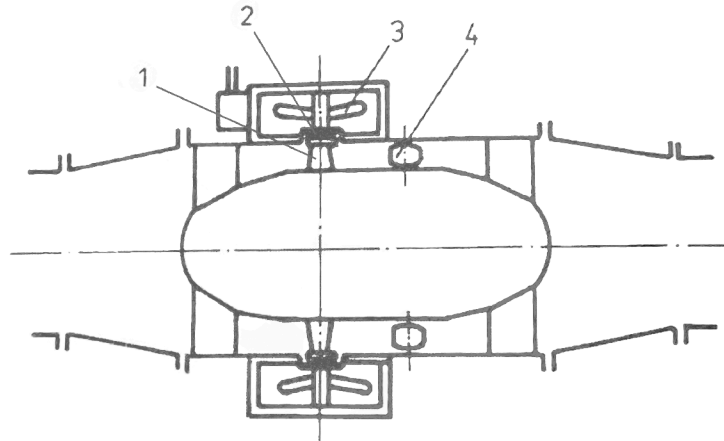
turbine has yet been used for PRV harvesting.

Without the usage of seals, magnetic inserts are inserted into the tips of blades and magnetic flux travels through the water filled gap [2]. The friction losses of turbulent water travelling through the gap can add up to even 10% of the generated power and are a function of tangential velocity [12]. Water contamination is another big problem, little particles of the contaminants can get stuck in the gap and damage the moving parts. Potentially catastrophic failure can occur by water corroding the stator windings and short circuiting the whole generator [12]. On the other hand the sealing problems are completely avoided.

3.3 Counter rotating runners

A fairly new design concept for energy harvesting is a turbine with counter rotating runners. It is an 2-stage axial turbine, where the runners are rotating against each other. Regulation is done trough controlling the velocity of the individual runners by frequency inverters, no mechanical regulation is needed. Efficiencies of up to 90 % have been achieved in numerical model simulations [13]. Big advantage of this system is possibility of in-line installation which saves civil costs.

Since at the inlet there is always axial flow, it is apparent that in first runner c_{u1} is zero, from equation 2.7 we see that the first runner's power output is dependent only on the tangential component of absolute velocity in the opposite direction (hence the minus sign) at the outlet . On the other hand, at the second runner at the inlet there is no longer only axial flow, for best efficiency the absolute velocity component c_{u2} at the outlet is close to zero. The goal in designing this type of turbine is to angle the blades such as that at the outlet we have only axial flow. Under constant flow conditions we can see the velocity



1 – Rotor blades, 2 – Stator-rotor gap, 3 – Generator stator, 4 – Guide vanes

Figure 9: Cross-section of a variation of STRAFLO turbine; adjusted according to [2]

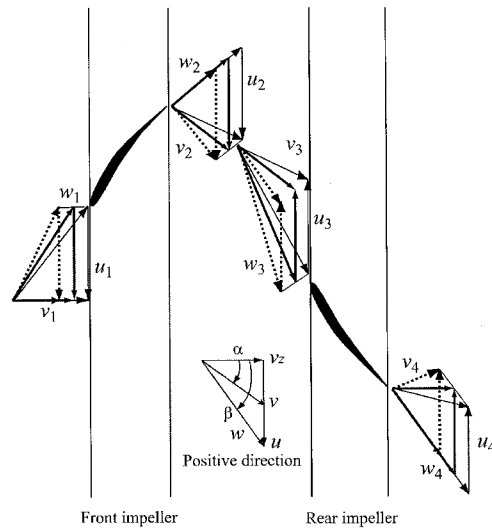


Figure 10: Velocity triangles for a turbine with counter rotating runners [14]

triangles with full thick lines in Figure 10 this is the BEP [14]. Under variable conditions the dotted lines and full thin lines represent less and more than optimal flow rate respectively and we can see that under variable conditions we no longer have only axial flow at the outlet in Figure 10. This is where regulation is needed, in velocity triangles the rotational velocity of a runner is represented by the u component, with controlling this variable by the means of a frequency inverter, we can almost always achieve axial flow at the outlet [14]. We can see this visualized in Figure 11 where for three different angles of α_1 the outlet flow v_4 has no circumferential component.

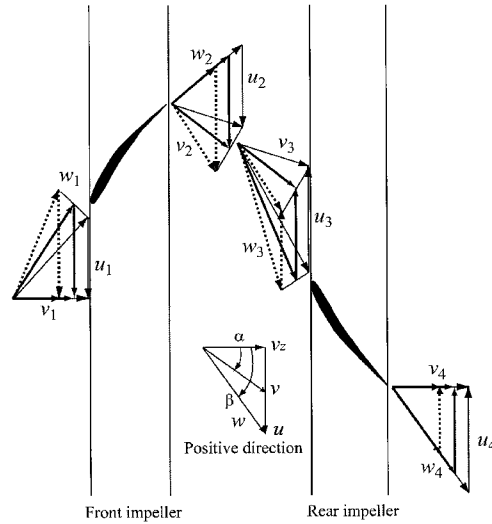


Figure 11: Velocity triangles of a regulated turbine under variable conditions [14]

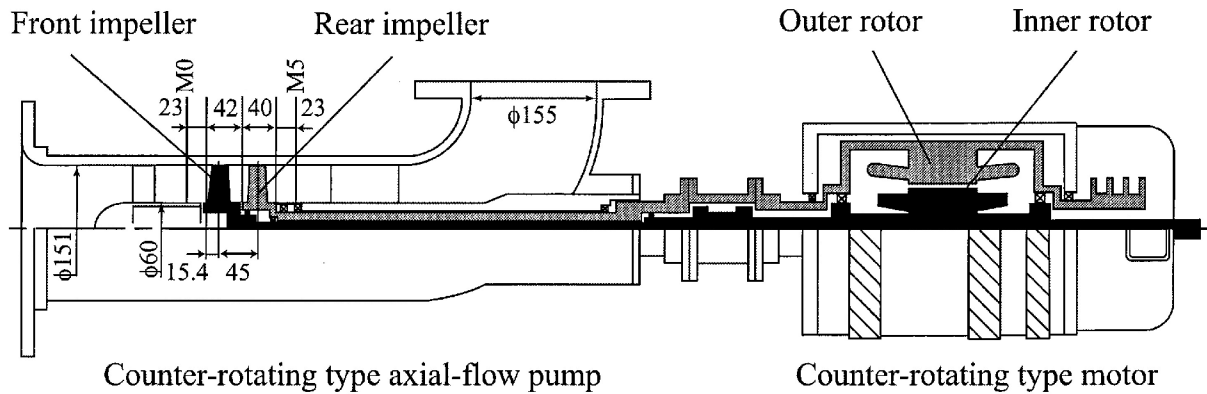


Figure 12: Semi-section view of counter rotating turbine and generator [14]

With having two counter rotating shafts there arises a problem with electrical generation. Researchers from Kyushu Institute of Technology came up with an innovating new electrical motor with counter rotating rotors, in Figure 12 it can be seen that the first runner is connected to the inner rotor with regular shaft and the outer rotor with a hollow one [14].

When two rotors are rotating opposed to each other, the resulting effective rotational velocity for electric power generation is the sum of both rotational velocities [14]. When installing a turbine, rotational velocity of a generator is dependant on the frequency of the power supply in use. This means that the effective rotational velocity is constant but the individual runner velocities can be regulated [14]. Experiments verified that even for uneven rotational velocities, the torque on a inner rotor is the same as on the outer one [14]. This has the advantage that the motor rotors counter balance them self and don't need additional supports [14]. There is also no disturbance to the flow at the inlet which preserves its efficiency. On the contrary the cost of the motor would be very high and the technical complexity would be a problem for reliability.

Another solution is with installing the turbine in a double elbow pipe, where the rotating shafts are brought out at the corners and each shaft has its own generator [15].

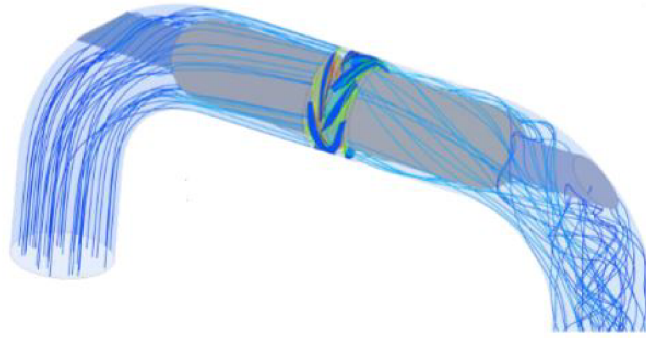


Figure 13: View of the double elbow variant [15]

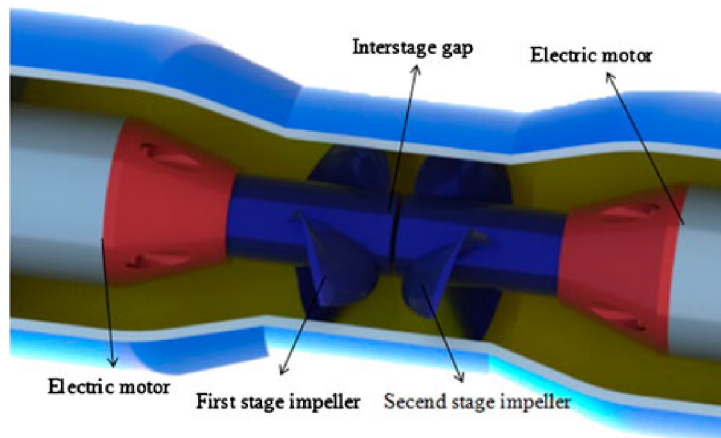


Figure 14: Schematic section view of bulb variant [16]

This solution is quite simple and cheap since we can use regular generators, but compared to the other ones it has its own disadvantages. Firstly we lose the in-line installation savings, secondly by using elbow pipes we introduce turbulence to the flow which reduces efficiency.

The third option, the most simple one is a "bulb" variant. Each turbine has its own generator, the whole electrical system is housed inside a bulb in front and behind the turbine for the first and second runner respectively [16]. In-line installation is preserved, no expensive motors are required and the flow at the inlet and outlet is not disturbed. The counter rotating turbine concept has only been tested in laboratories and isn't used in any location, but the research still continues and it is a promising new concept.

3.4 Spherical lift turbine

Spherical lift turbine is inspired by vertical axis wind turbines that utilize lift force acting on an aerofoil [17]. All these turbines are vertical axis turbines, that means that flow is always perpendicular to the turbine axis.

They use aero foiled shaped blades arranged in a spherical shape to make it fit onto a pipe and while also having a helical curve. The helical curved blades help with even torque distribution in a way that there is always a aerofoil section in every possible angle of attack [18] Vertical axis turbines are notorious for their problems with not being able to self start [18]. NACA aerofoils are used thanks to their very detailed characteristics

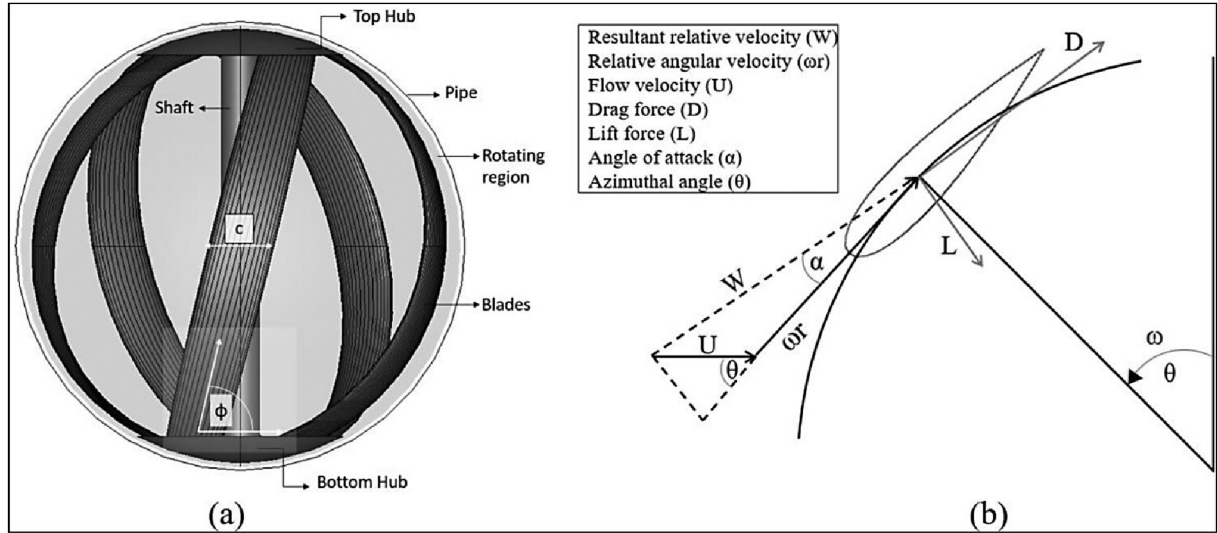


Figure 15: Forces acting on the aerofoil [18]

and good lift to drag coefficients.

Efficiencies around 25-30% have been achieved[18], where efficiency is defined as:

$$\eta = \frac{M_k \omega}{\rho Q \Delta E} \quad (3.1)$$

Important parameters that influence the performance of lift based turbines are rotor solidity σ and the tip velocity ratio (TSR). Rotor solidity is a dimensionless parameter defined as a ratio of a frontal blade area and a theoretical disk area, basically how closely the rotor represents a full disk and is defined as

$$\sigma = \frac{Nc}{\pi D} \quad (3.2)$$

Where N is the number of blades, c is the chord length and D is the diameter of rotor [18]. TSR is a ratio of tangential velocity of the blade tip and the velocity of flow, it is defined as

$$TSR = \frac{\omega D}{2U} \quad (3.3)$$

Where ω is the angular velocity and U is the velocity of flow[18].

Low values of TSR tend to lead to stalling and very high values lead to high stresses in the blades that can facilitate a structural failure. Finding the best combination of these parameters is key to reaching high power extractions [18]. 4 turbines with a capacity of 200 kw have been installed in Portland, Oregon in the US by a company called Lucid Energy [17].

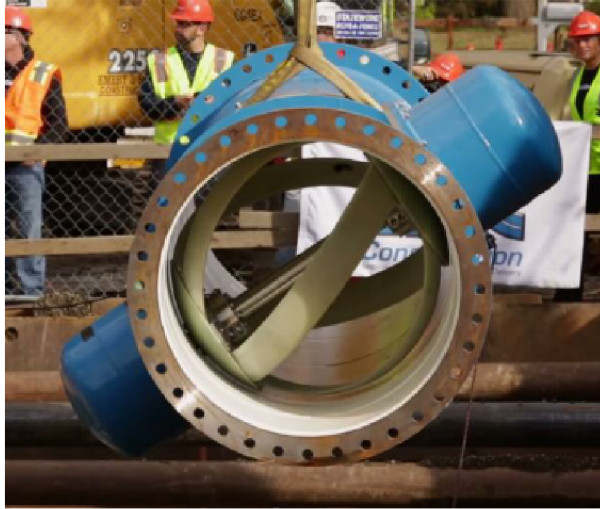


Figure 16: Lucid energy turbine [17]

4 Turbine design

4.1 Basic parameters

Design of the turbine is for a specific location, Ferlach a small town in Austria which uses water's potential energy to deliver it to the water distribution network. Measurements have already been realized and these are the presented data.

Flow rate $Q = 15l/s$ and Head $h = 50m$. The operating velocity of the runner is set by the frequency of the grid which is $50Hz$ from that the rotational velocity is given as $n = 3000 \frac{1}{min}$. Pipes used have a diameter of $D = 100mm$, that restricts the outer diameter selection, inner diameter $d = 90mm$ is chosen, since the radial distance between the diameters is small making an assumption that the flow characteristics stay the same in the radial direction can be done with little error. First the turbine efficiency needs to be predicted, similar turbines achieved efficiencies of around 70%. Efficiency is set as $\eta = 0.7$. Now the theoretical power can be computed.

$$P = \rho g Q H \eta = 5,15kW \quad (4.1)$$

4.2 Approach to turbine design

There are multiple ways to approach turbine blade design, from complete 3D model simulations to 2D blade section simulation. The 3D approach is vastly more complicated and numerically difficult which would be unreasonably complex for a bachelor thesis, in next chapters the design and examination will only be in 2D. But there still arises a problem of displaying a cylindrical surface in a plane. Conformal transformations is used, this transformation method preserves angles and ratios of length, visualized in Figure 17.

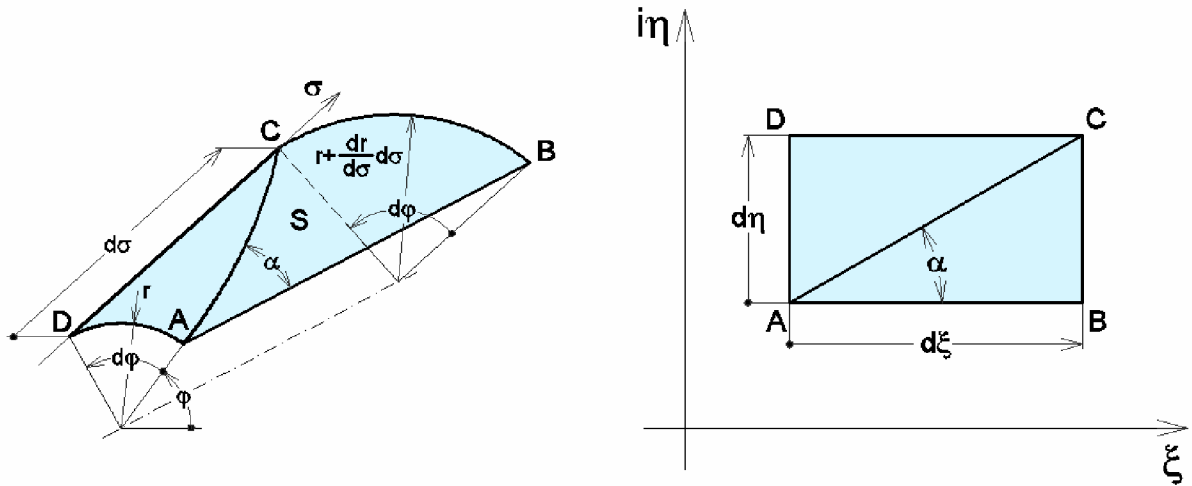


Figure 17: Conformal transformation [19]

4.3 Angles β_1 and β_2

The leading edge of the turbine is splitting the flow into a pressure and suction side. The angle of the leading edge β_1 is to be designed as to primarily avoid creating a shock component of velocity, this would negatively affect the efficiency. Angle β_2 mainly affects the amount of energy that is extracted from the flow.

For simplicity the angles won't change along the radial direction. Since the flow rate and cross sectional area are known, from the continuity equation absolute velocity at the inlet c_1 can be computed, $c_1 = c_{1m}$ can also be written since the flow is axial.

$$c_1 = \frac{Q}{S} = \frac{Q_4}{\pi(D^2 - d^2)} \quad (4.2)$$

Tangential velocity u_1 can be determined from the velocity of the rotating runner and its diameter.

$$u_1 = \pi D n \quad (4.3)$$

By using the Pythagoras theorem w_1 is expressed as

$$w_1 = \sqrt{c_1^2 + u_1^2} \quad (4.4)$$

With all velocities at the leading edge determined β_1 can be expressed as

$$\beta_1 = \arctg\left(\frac{u_1}{c_1}\right) \quad (4.5)$$

Tangential velocities are the same at the inlet and the outlet since the diameter and the runner velocities are the same, the following equation can be written

$$u_1 = u_2 \quad (4.6)$$

From the Euler turbine equation the tangential component of absolute velocity c_{u2} at the outlet is expressed as

$$c_{u2} = -\frac{gH\eta}{u_2} \quad (4.7)$$

Again using the Pythagoras theorem absolute velocity c_2 is expressed

$$c_2 = \sqrt{c_{m2}^2 + c_{u2}^2} \quad (4.8)$$

Relative velocity at the trailing edge is given by

$$w_2 = \sqrt{(c_2 + u_2)^2 + u_2^2} \quad (4.9)$$

And finally β_2 can be computed

$$\beta_2 = \arctg\left(\frac{c_{u2} + u_2}{c_{m2}}\right) \quad (4.10)$$

4.4 Camber line

Now that all angles have been determined the two points need to be connected to create a camber line. There are multiple methods by which this can be done, there is the linear change of angle β , quadratic change of angle β and the linear change of $tg(\beta)$. For simplicity the linear change of angle β is used.

Equation for a line can be written for β .

$$\beta = a\xi + b \quad (4.11)$$

After conformal transformation, angle β can also be expressed as

$$\tan(\beta) = \frac{d\eta}{d\xi} \quad (4.12)$$

When separating the variables and by combining the equations 4.11 and 4.12 we get

$$\tan(a\xi + b)d\xi = d\eta \quad (4.13)$$

Integration is applied to both sides

$$\int_{\xi_0}^{\xi} \tan(a\xi + b) d\xi = \int_0^{\eta} d\eta \quad (4.14)$$

After integration

$$-\frac{1}{a} \ln(\cos(a\xi + b)) + c = \eta \quad (4.15)$$

By applying these boundary conditions the leading edge starts in the middle of the coordinate system

$$\xi = 0; \eta = 0 \quad (4.16)$$

From there the first constant c can be expressed as

$$c = \frac{1}{a} \ln(\cos(+b)) \quad (4.17)$$

Boundary conditions for both angles β_1 and β_2 are

$$\beta = \beta_1; \xi = 0 \quad (4.18)$$

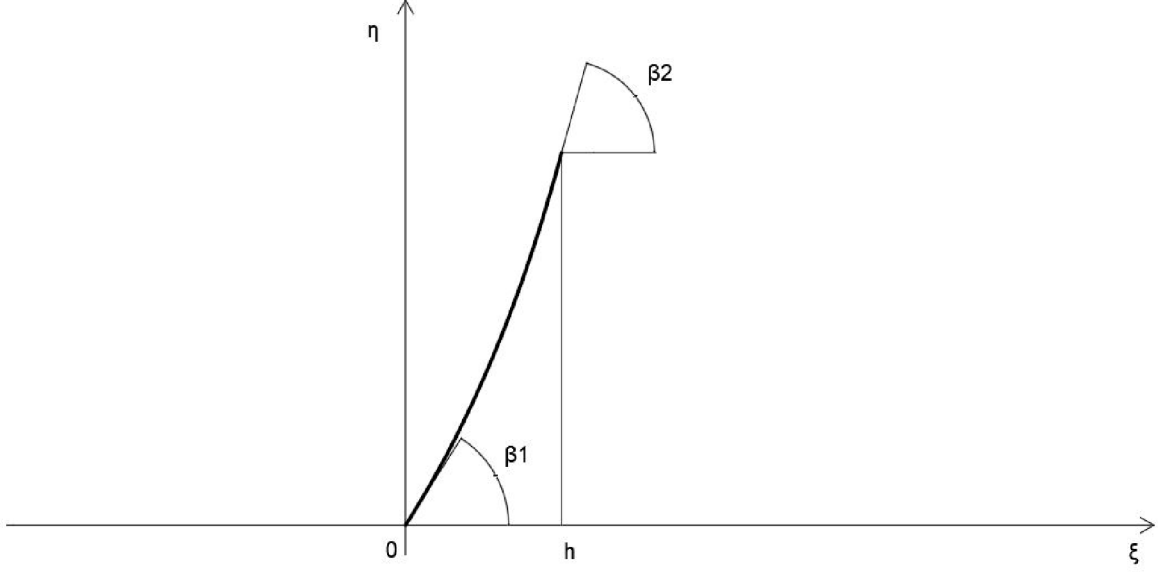


Figure 18: Camber line in conformal coordinates

$$\beta = \beta_2; \xi = h \quad (4.19)$$

Where h is the depth of the turbine.

By applying these boundary conditions into the equation 4.11 the following constants are acquired

$$a = \frac{\beta_2 - \beta_1}{h} \quad (4.20)$$

$$b = \beta_1 \quad (4.21)$$

After applying the constants to the equation 4.15 the function governing the camber line is finally acquired

$$\eta = \frac{1}{a} \ln\left(\frac{\cos(b)}{\cos(a\xi + b)}\right) \quad (4.22)$$

4.5 Blade thickness

When designing a turbine blade geometry, it is favourable to use the data from aerofoil design, particularly the NACA aerofoils. This was an American state agency and a precursor to NASA that thoroughly tested a large set of aerofoils. The first set of aerofoils they tested were specified by four digits, also called the four digit series, for example NACA 2412, where the first digit describes the maximum camber as percentage of chord, the second digit describes the distance of maximum camber from the aerofoil leading edge in tenths of chord and the last two digits describe the maximum thickness in percentage of chord.[20]

On of the more basic and symmetric aerofoils will be used the NACA 0012 symmetric aerofoil. Its thickness distribution is defined as

$$y_T = \frac{T}{0.2} (a_0 x^{0.5} + a_1 x + a_2 x^2 + a_3 x^3 + a_4 x^4) \quad (4.23)$$

Where individual constants are defined as

$$a_0 = 0.2969; a_1 = -0.126; a_2 = -0.3516; a_3 = 0.2843; a_4 = -0.1036 \quad (4.24)$$

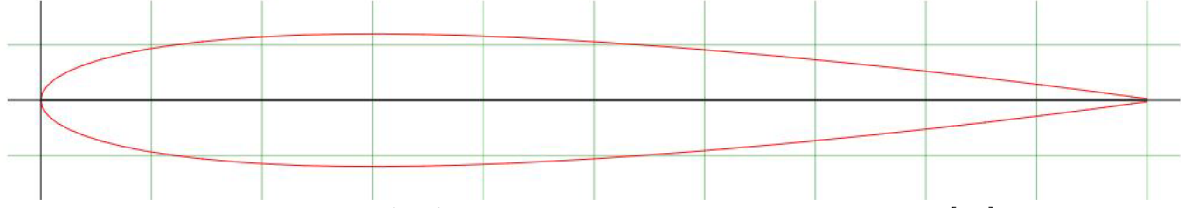


Figure 19: NACA 0012 aerofoil thickness distribution [21]

for a closed trailing edge

4.6 Giving thickness to the camber line

Now that the thickness distribution is defined it needs to be applied to a camber line based on its curvature, this is done by differentiating the camber line function, this is possible since the camber line function is continuous throughout the whole interval. From there the angle of the curvature can be extracted from the derivative at every point, afterwards by using trigonometry functions the functions for the upper and lower surfaces of the turbine blade are defined.

For angle θ can be written

$$\theta = \text{atan}\left(\frac{d\eta}{d\xi}\right) \quad (4.25)$$

In the previous chapters linear change of angle β was used, its derivation will be a constant and for angle θ we can write

$$\theta = a\xi + b \quad (4.26)$$

Equations for upper and lower surface will be defined as

$$\eta_u = \eta + \cos(\theta)y_T \quad (4.27)$$

$$\eta_l = \eta - \cos(\theta)y_T \quad (4.28)$$

$$\xi_u = \xi + \sin(\theta)y_T \quad (4.29)$$

$$\xi_l = \xi - \sin(\theta)y_T \quad (4.30)$$

This can be visualized in Figure 20.

After the equations are plotted geometry profile of a turbine blade is acquired, this can be seen in Figure 21. The last thing modified in geometry will be the trailing edge, to avoid the creation of Karmann vortex street which would cause structural vibration and eventually a fatigue failure. The trailing edge will be cut short with a 30° angle, with experiment it was shown that this is the critical value at which the vortex amplitudes are at its lowest.

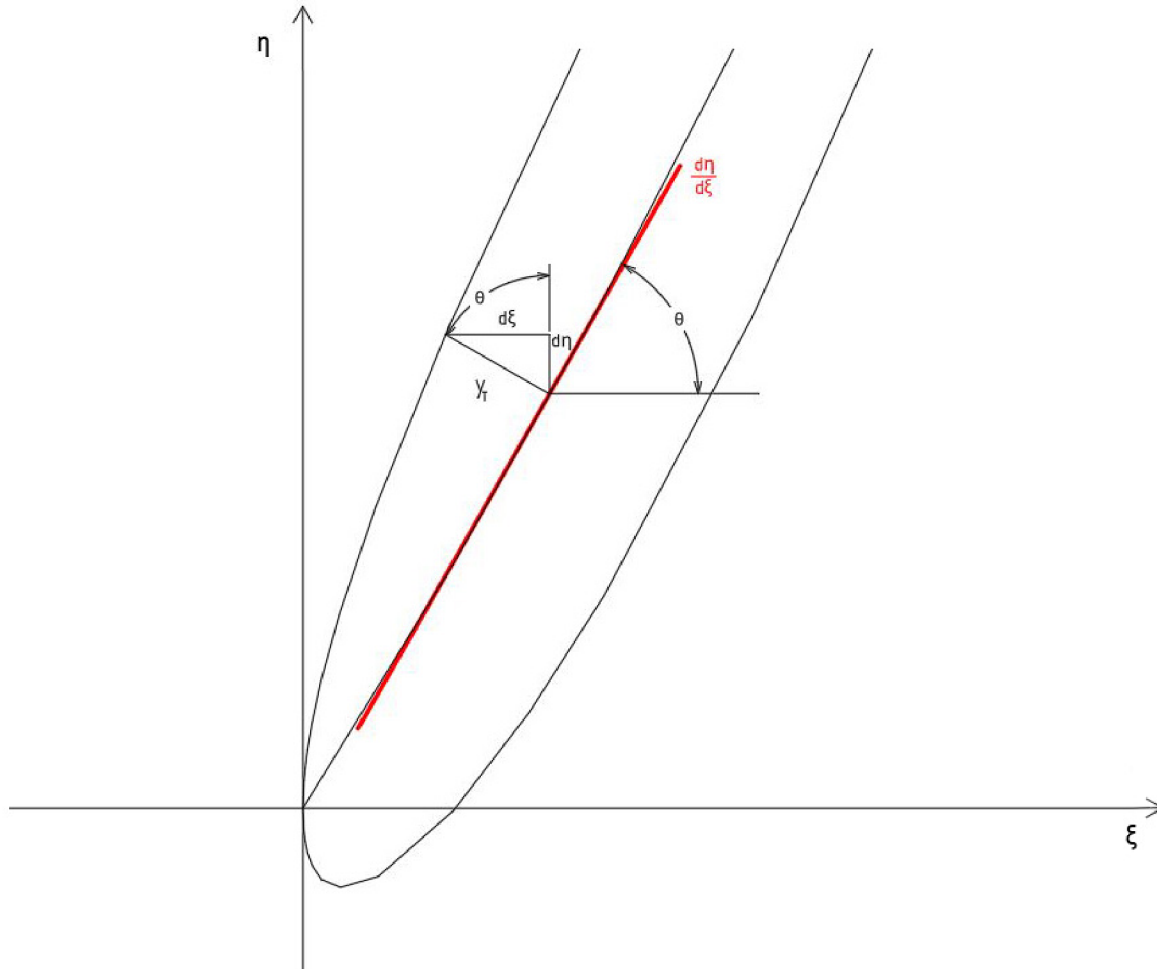


Figure 20: Visualisation of applying thickness to the camber line

5 CFD simulation

5.1 Creating geometry using CAD

Next step will be creating a geometry of a rotating channel in on of the CAD software's, exporting it into a STEP file and uploading it into Ansys Fluent. Autodesk Inventor was chosen as the CAD software. Since the rotating channel will be periodic, periodic boundary conditions can be used and only one blade needs to be modeled.

5.2 Creating the mesh

After exporting the geometry into Ansys, a mesh needs to be created to discretize the continuous geometric space and evaluate pressure and velocity in each cell. There are two choices when it comes to creating a mesh, either a structured mesh which has regular connectivity between neighbouring cells, this type of mesh saves space and has better convergence characteristics on the other side for a complex geometry it may not be possible to create this type of mesh. Unstructured mesh is more suitable for complex geometry

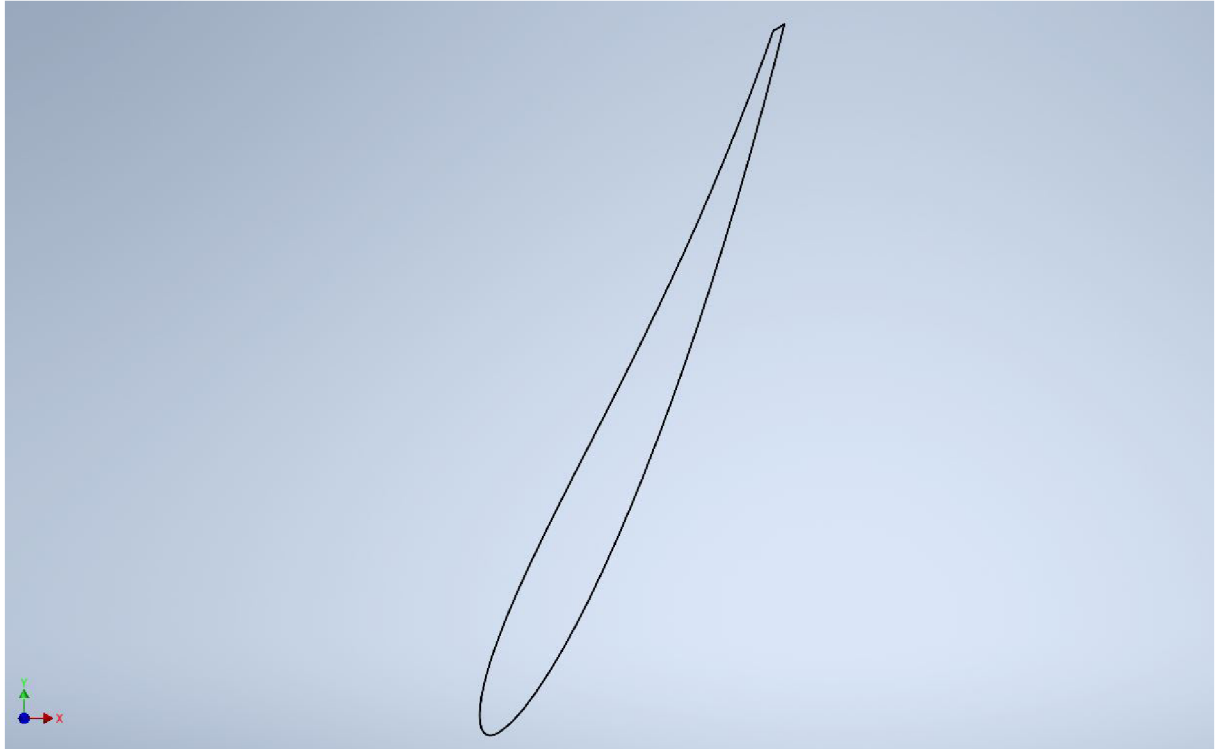


Figure 21: Geometry profile of the turbine blade in 2D

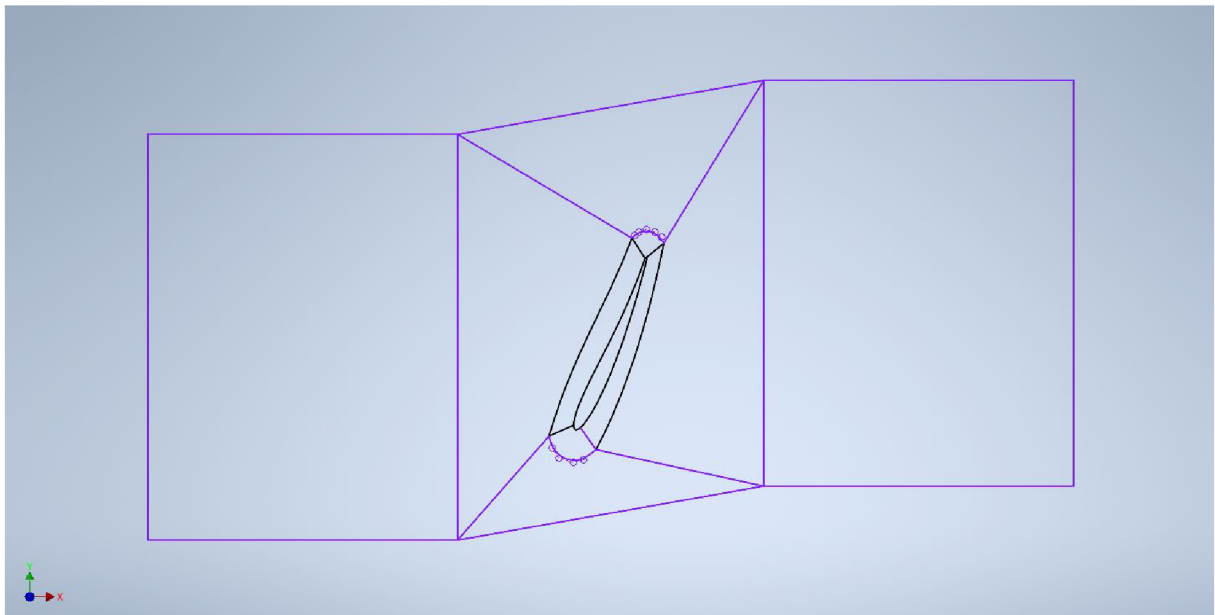


Figure 22: Geometry of the channel in conformal coordinates

with the drawback of being more space inefficient. In CFD when possible it is always preferred to create a structured mesh, this is the type that will be chosen.

The blade is surrounded by an envelope with the aim of applying finer mesh to this region around the surface of the blade to capture the steep velocity gradients caused by the no-slip condition. When evaluating the quality of a mesh in the near wall region a dimensionless parameter y^+ is used. It is defined as

$$y^+ = \frac{yu_t}{\nu} \quad (5.1)$$

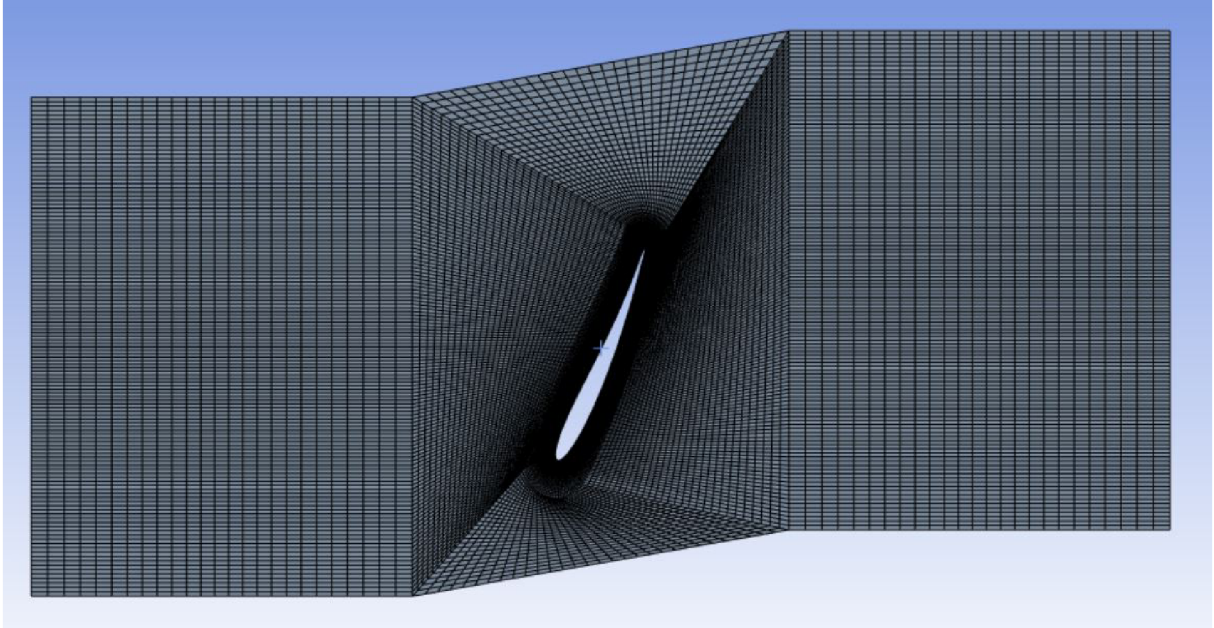


Figure 23: Structured mesh of the first iteration

where y is the distance from the wall, ν is the kinematic viscosity and u_t can be expressed as $u_t = \sqrt{\frac{\tau_w}{\rho}}$ where ρ is the density and τ_w is the wall shear stress and can be expressed as $\tau_w = \mu \frac{\partial u}{\partial y}$ where μ is the dynamic viscosity and u is the flow velocity[22]. It is a non dimensional parameter representing the distance of the first cell from the wall. Recommended values of y^+ depend on the turbulence model used, for the first iteration we will use a realizable k-epsilon turbulent model which is insensitive to the y^+ values.

In the Figure 23 can be seen, sizing with bias was placed on the inner edges of the envelope to create a finer mesh close to the boundary layer. Since the upper and lower walls will be periodic they need to have the same number of nodes, sizing with the number of divisions was used and to ensure the same number of cells, hard behaviour was needed. Named selections were created for surfaces and edges to afterwards be able to assign them the needed boundary conditions, seen in Figure 24. The mesh is afterwards uploaded to Ansys Fluent.

5.3 Fluent setup

The first thing to choose is if the flow changes in time, that means is steady or transient, with the first iteration we have no way of knowing that until we run it in transient mode. For simplicity a steady state will be assumed. For the type of solver there are two options, pressure and density based, density based solvers are mainly for high velocity compressible flows, the pressure based on the other hand is more suitable for flows where we can assume it is incompressible. Thus the pressure based solver is more suitable for this application. As said in the previous chapter, for the first iteration the k-epsilon turbulence model will be used.

Boundary conditions will be the velocity at the inlet, which we will be derived from the continuity equation, translational velocity of the rotating rotating channel which is

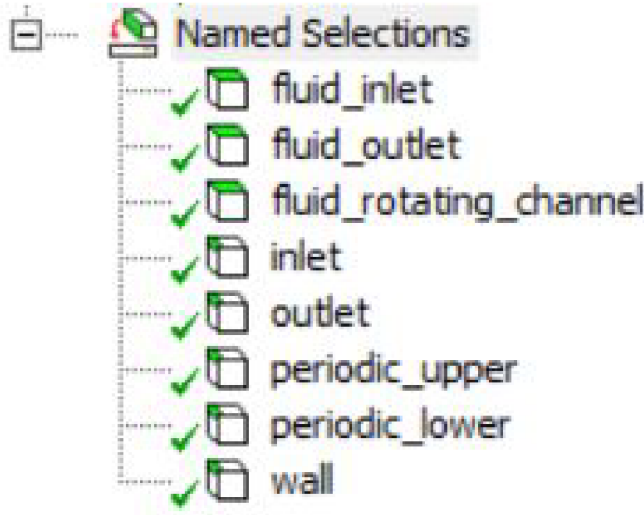


Figure 24: Named selections

from the expression $u = 2\pi nr$ where n is the rotational velocity and r is the radius of the turbine. At the upper and lower edge the periodic boundary condition will be applied, at the surface of the turbine blade the no slip condition needs to be applied. Since Ansys Fluent cant run a purely 2D simulation we need to select the depth of the channel which will be 5 mm. Finally after initialization the simulation can be started.

5.4 Postprocessing

First thing to check is if the flow is splitting at the leading edge, for that we need to display the streamlines. In Figure 25 it can be seen that the flow is split pretty close to the leading edge, in the next iteration the angle β_1 should be decreased. Next there is a need to calculate how much energy has the turbine utilized from the flow. When flow rate is assumed to be constant, it is apparent that the only type of energy of the flow consumed is the pressure energy. Pressure energy from the flow can be expressed by comparing the pressure at the inlet and the outlet by the following equation.

$$E = \frac{p_1}{\rho} + \frac{v_1^2}{2} - \frac{p_2}{\rho} - \frac{v_2^2}{2} \quad (5.2)$$

To get the energy in terms of head the Equation 5.2 needs to be divided by the gravitational constant g . Afterwards the efficiency of the turbine will be examined. Efficiency of a turbine is defined as

$$\eta_T = \frac{M_k \omega}{\rho Q E} \quad (5.3)$$

where M_k is the torque, ω is the angular velocity of the turbine and is known from the rotational velocity n , E is the energy extracted from the flow, Q is the flow rate and ρ is the density of the fluid. Torque can be expressed as

$$M_k = FR \quad (5.4)$$

Where the force is given by the following equation.

$$F = \iint_S (-p + \tau) dS \quad (5.5)$$

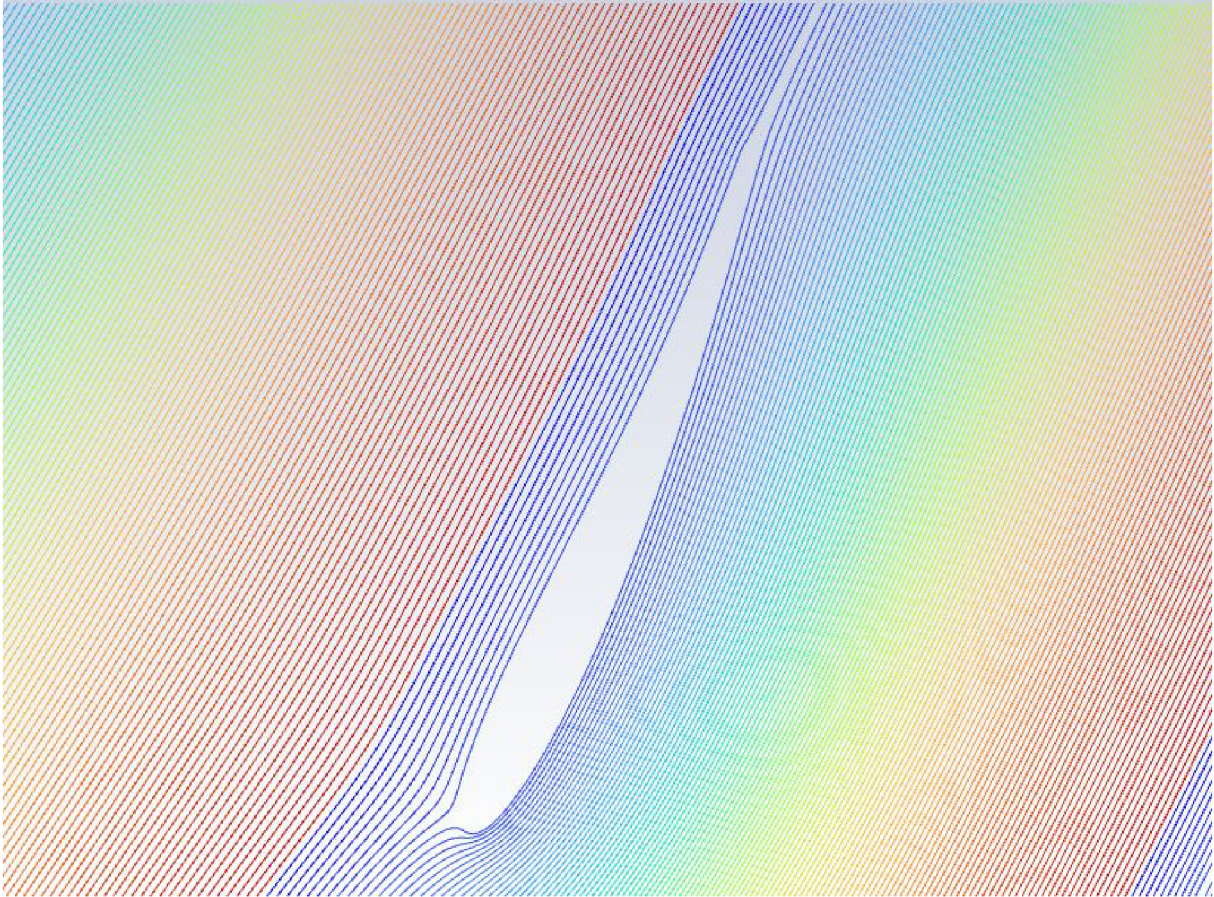


Figure 25: Streamlines in the rotating channel

This is computed by Ansys. There arises a problem that the force F acting on the turbine blade is not constant along the radius R . The correct course of action would be to integrate the force along the radius by the following equation.

$$M_k = \int_0^R F_{(R)} dR \quad (5.6)$$

For the specified pipe dimensions where the ratio of pipe diameter and the turbine hub is close to 1 a small error will be made with the presumption of a constant Force along the radius.

5.5 Conclusion after the first iteration

First by using the Euler turbine equation the angles β_1 and β_2 can be computed.

$$\beta_1 = 57.4^\circ \quad (5.7)$$

$$\beta_2 = 75.0^\circ \quad (5.8)$$

Afterwards the two points were connected by using the Equation 4.22 and thickness distribution of NACA 0012 was applied. The number of blades z was chosen.

$$z = 3 \quad (5.9)$$

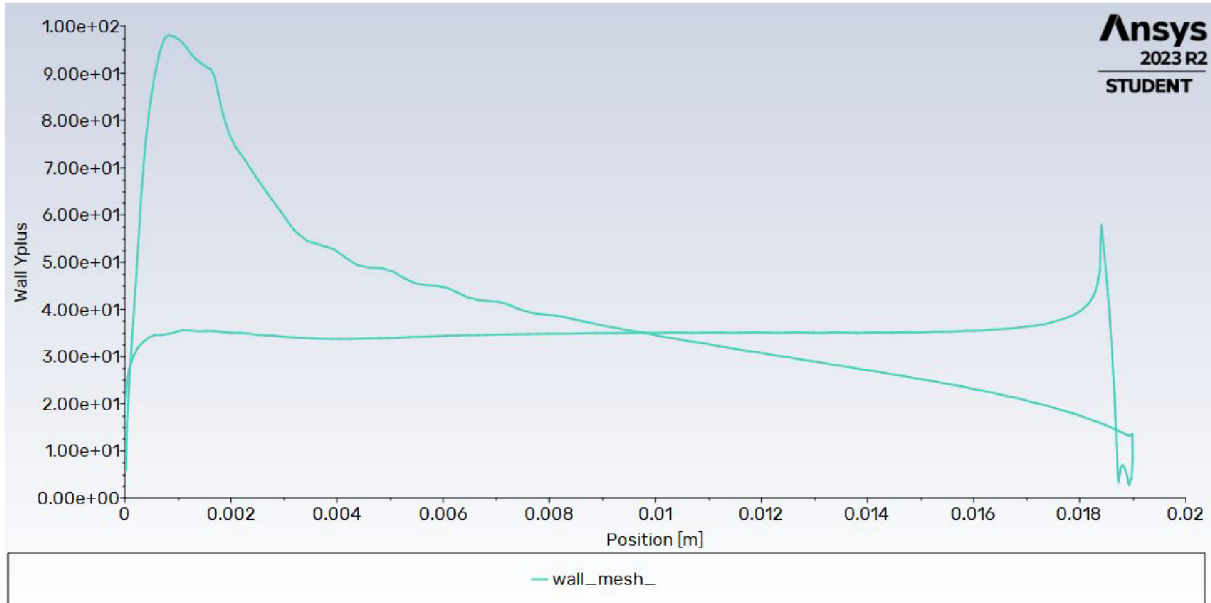


Figure 26: Plot of $y+$ parameter around the surface of the blade

The height of the rotating channel l was determined by using the following equation.

$$l = \frac{\pi \frac{D-d}{2}}{z} \quad (5.10)$$

After running the simulation the utilized head is calculated and it is 9,3 meters. This means that it was only managed to use approximately 18,6% of the available head which is not ideal, it is always best to use all the available energy.

There are two ways to correct this in the next iterations, more blades can be added to the turbine which will extract more energy from the flow or the sweep of the blade can be increased, this subsequently increases the depth of the turbine. The first solution is preferred since the compactness of the turbine is also a parameter that needs to be kept in mind. After utilized energy has been calculated, in Fluent the force creating the torque can be plotted and from there the efficiency of the turbine can be computed.

$$\eta = 77\% \quad (5.11)$$

This number is relatively close to the efficiency predicted but due to our simplified simulation approach losses mainly from the runner and chamber gap and many others were neglected, in reality lower efficiencies should be expected. In Figure 26 the plotted $y+$ parameter around the surface of the turbine blade can be seen, it varies widely and even reaches the values of 100, for the chosen turbulence model this is fine.

5.6 Second iteration

In the next iterations a different turbulence model will be used. The turbulence model chosen strongly depends on the type of flow being considered. The k-epsilon model, used in the first iteration is best suited for a free stream region far away from the wall with no flow separation. In the near wall region this model uses so called wall functions to predict

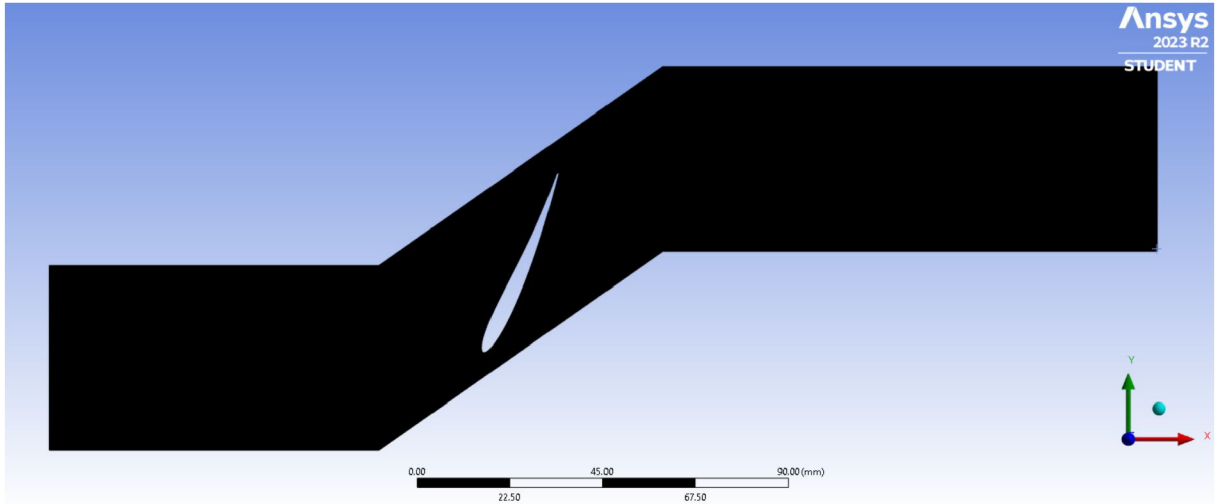


Figure 27: Structured mesh of the second iteration

the flow and doesn't compute it directly.

In turbo machinery CFD the most important region to accurately capture is the boundary layer, from this region we calculate all the important characteristics like lift and drag forces and efficiency. The model that best captures this region is the SST k-omega turbulence model which computes it directly, but to be able to effectively use this model there are a few guidelines that should be adhered to regarding the mesh. The y^+ parameter should be less than 5 and ideally close to 1, by doing this the best results are achieved. To better utilize the available head larger number of z will be chosen.

$$z = 7 \quad (5.12)$$

The only change this makes to the geometry is that the height of the channel will be smaller, this can be seen in Figure 27. The first thing to check after running the simulation is if the desired y^+ values were achieved, this is calculated in the simulation so there is no other way to check this beforehand. The plot of y^+ can be seen in Figure 28, in it can be seen that the threshold value of 5 was achieved. Next the streamlines are displayed in Figure 27 to check where the flow is splitting in terms of the leading edge.

To check that the flow hasn't separated velocity in the X direction is plotted, from Figure 29b it is apparent that the boundary layer isn't separated. From the Equation 5.2 the utilized head is once more calculated, this comes to 68 % of the available head, a noticeable improvement. From the Equation 5.3 the efficiency is calculated.

$$\eta = 68\% \quad (5.13)$$

The lower calculated efficiency could be explained by bigger friction and form losses from adding a larger number of blades. Conclusion of the second iterations is that it is an improvement compared to the first one, in further optimization the geometry would be further revised, since there is no apparent flow separation angle β_2 could be enlarged to extract even more energy, the camber line curve could also be changed for a more complex one to achieve better results.

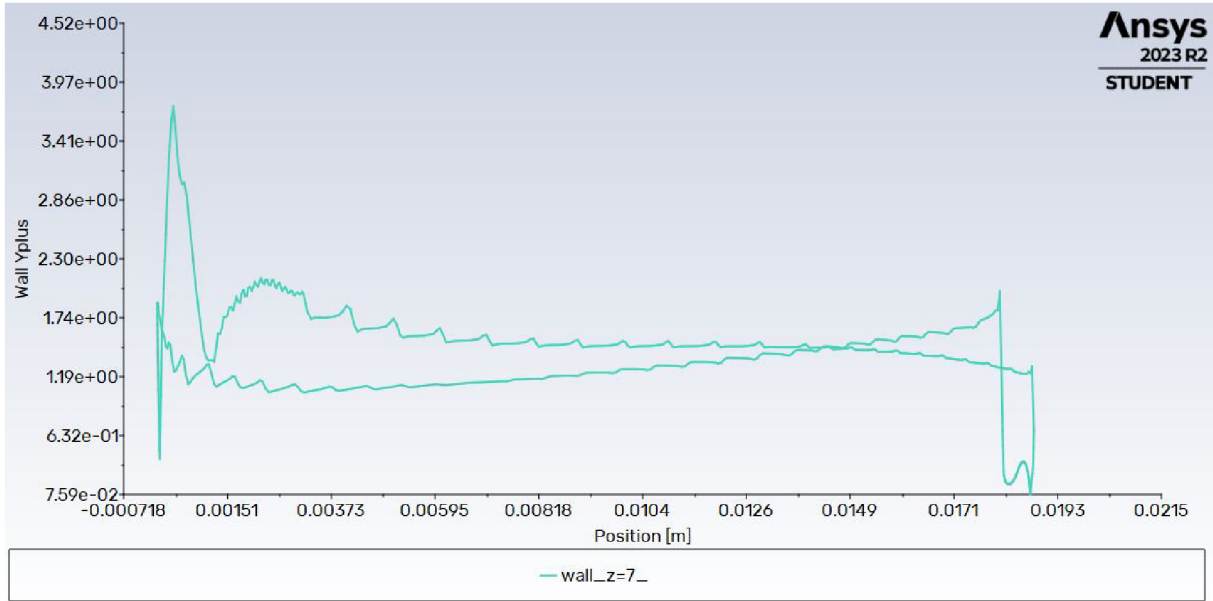
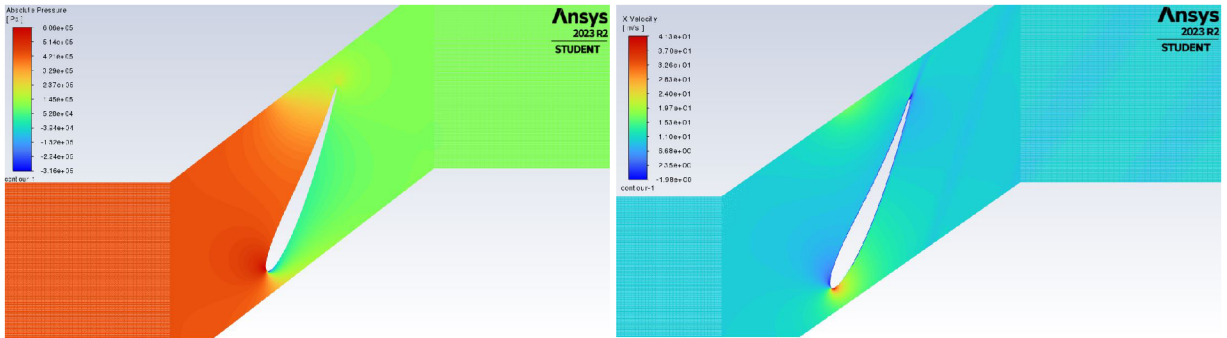


Figure 28: Plot of y^+ parameter in the second iteration



(a) Absolute pressure distribution of the second iteration (b) Contours of X velocity of the second iteration

Figure 29: Contours of second iteration

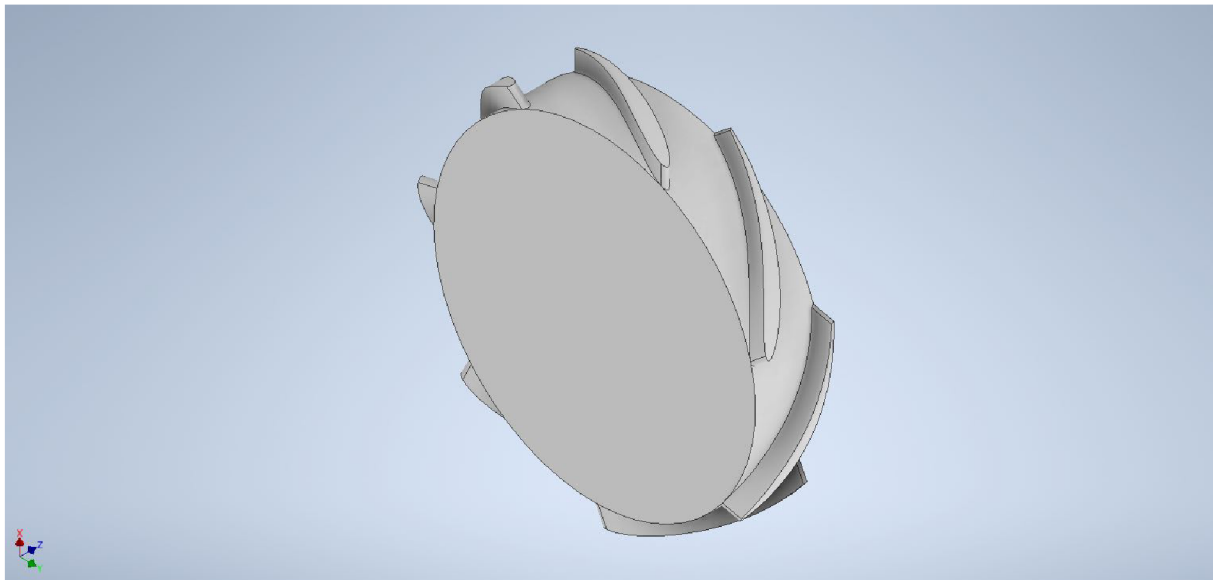


Figure 30: 3D model of the second iteration

5.7 Counter rotating turbine

In the third simulation and the last one we will try to imitate the counter rotating concept. This is with the aim to extract even more energy from the flow than in the previous iterations. From the Euler turbine equation it is apparent that the highest theoretical efficiency is achieved by having axial only outlet flow in the second runner, this means that the outlet velocity of the second runner has no tangential component.

The geometry of the individual blades will stay the same, only a second identical runner will be added behind the first one, the orientation will be different, this can be seen in Figure 31. One small update is the elongated outlet channel to better capture the wake of the blades. Next we will upload the geometry into Ansys fluent and create a structured

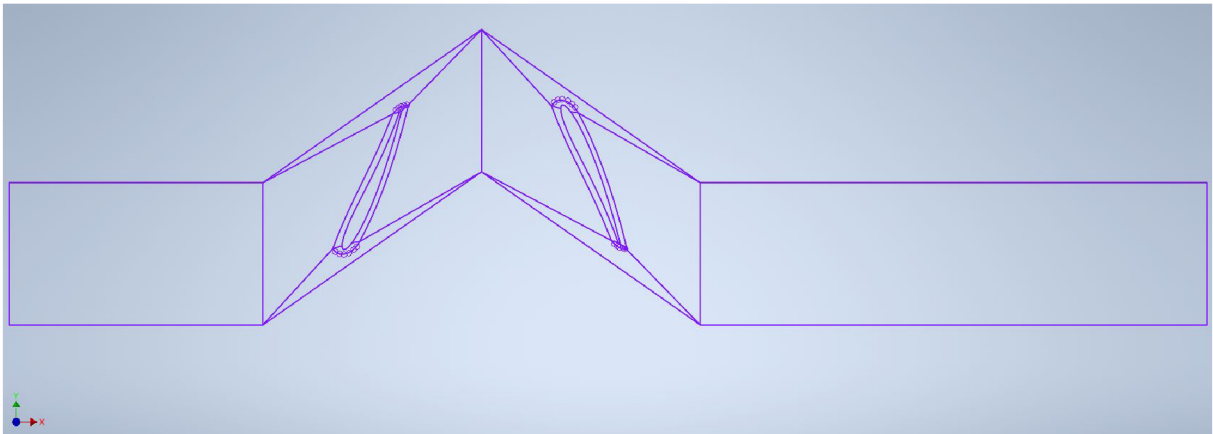


Figure 31: Rotating channel of the counter rotating turbine in Inventor

mesh and again try to adhere the required y^+ values to use the k-omega turbulence model. The boundary conditions will be the same as before with one exception, since the second runner will be rotating to the opposite side as the first one the translational velocity will be applied to the opposite side. After setting up the boundary conditions and initializing the simulation is started.

The post processing process will be the same as before, the first thing calculated is the head utilized, this equals $H = 101 m$, over two times the projected head. The turbine designed is creating too much resistance to the flow, the opposite problem faced in first iteration of the single stage turbine. The solution to this would be to decrease the number of blades z and or decrease the outlet blade angle β_2 .

When the streamlines are displayed in Figure 32 it is apparent that the flow is splitting at significant distance from the leading edge, this creates unnecessary hydraulic losses. Another thing that is noticed is the void of streamlines on the suction side of the blade in the second runner, this suggests flow separation. To check if the flow has really separated the velocity contours in the X direction are displayed in Figure 33. In the Figure 33 we can indeed see that the flow has separated on the second runner from the negative values of velocity. Flow separation comes with sudden loss of lift force, lower lift force means lower efficiency.

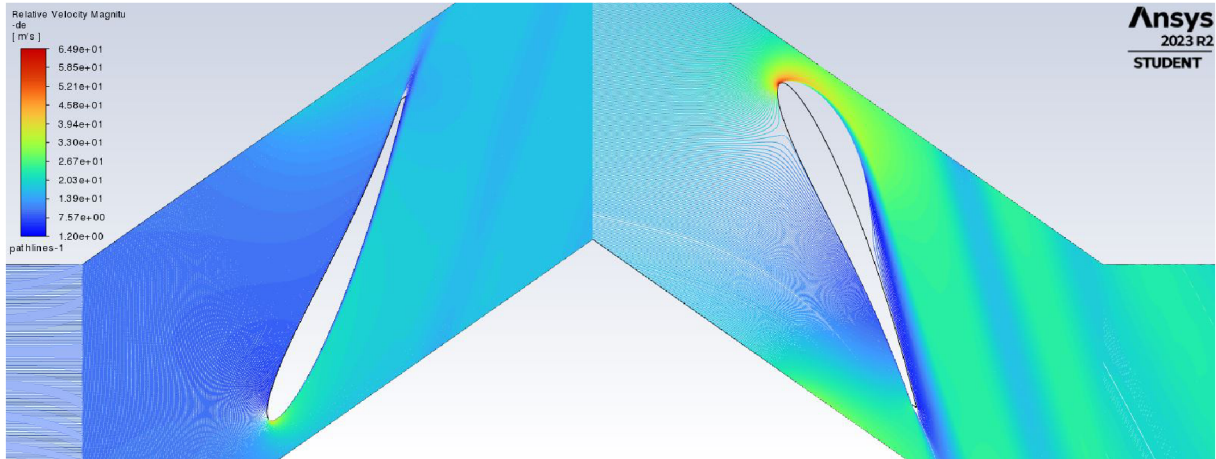


Figure 32: Streamlines in the counter rotating turbine

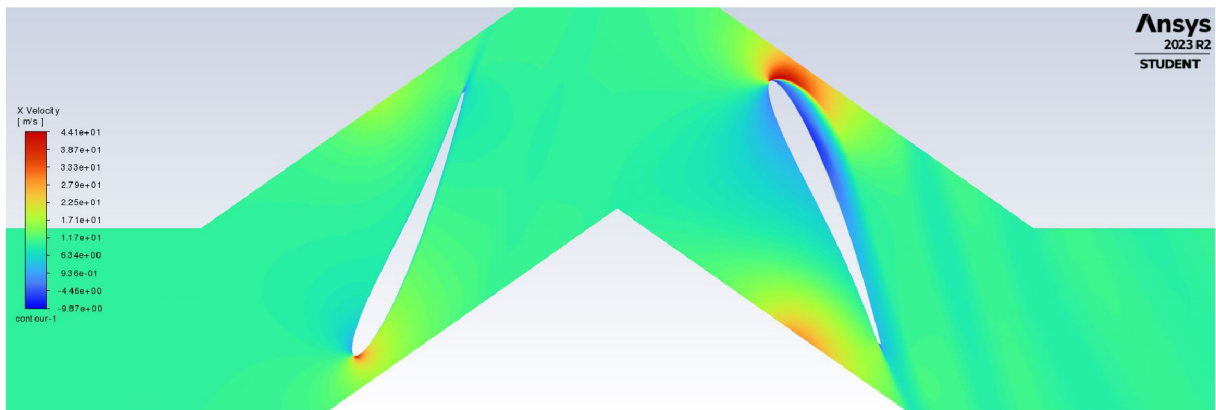


Figure 33: Velocity field contours in the x-direction of the counter rotating turbine

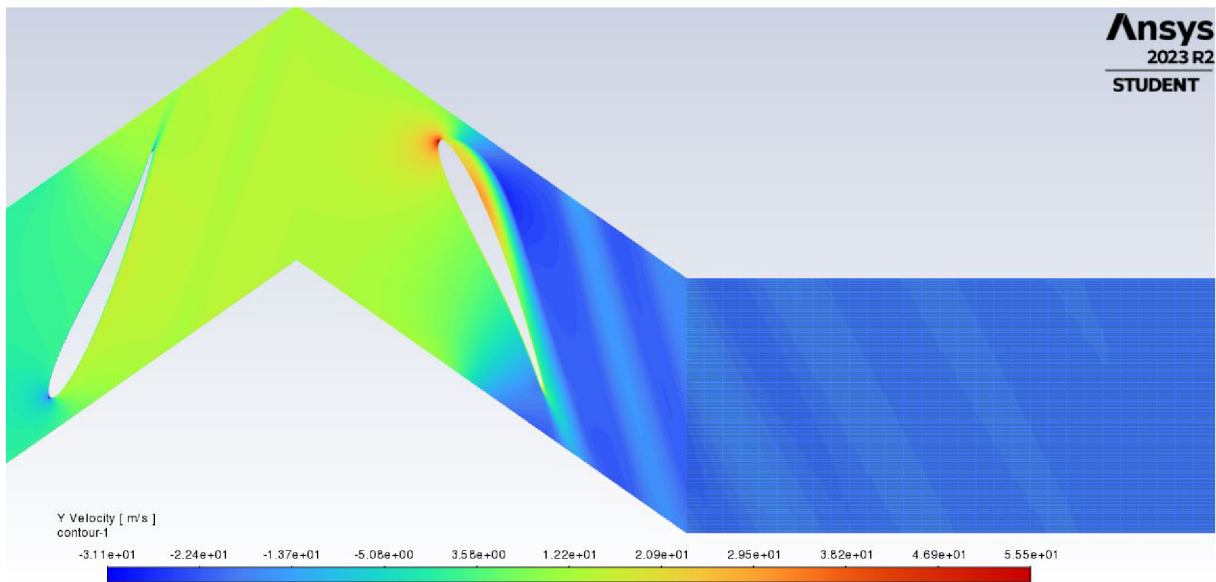


Figure 34: Velocity field in the Y-direction of the counter rotating turbine

Afterwards it is important to check if axial outlet flow has been achieved. For this velocity field in Y direction is plotted in Figure 34. If the flow is supposed to axial values close to zero should be expected, it can be seen in Figure 34 that this inst the case. To correct this and the flow separation lower values of angle β_2 would be chosen in the

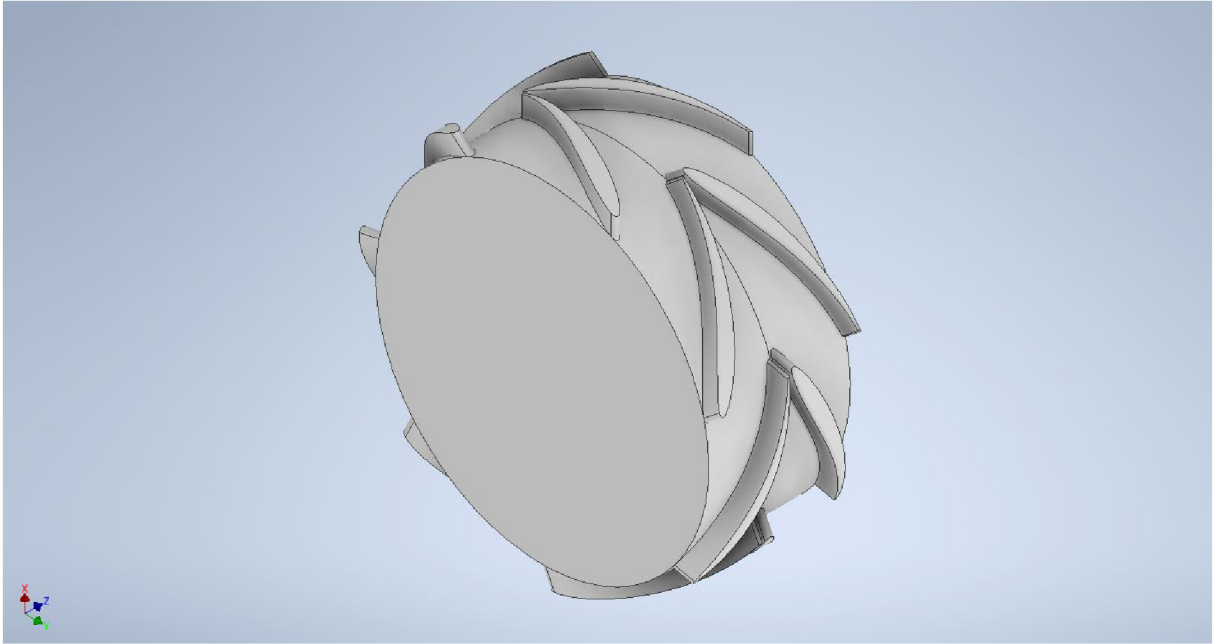


Figure 35: 3D model of the counter rotating turbine

-	number of blades z [1]	utilized head in [%]	efficiency η [%]
1. iteration	3	18.6 %	77 %
2. iteration	7	77 %	68 %
Counter rotating turbine	7	202 %	71 %

Table 1: Summary of final data from the CFD simulation

next iteration. By plotting the forces and summing the torque from both runners we can calculate the achieved efficiency.

$$\eta = 71\% \quad (5.14)$$

This is surprisingly high when we take flow separation into the account.

Conclusion

After a brief theoretical introduction, the first chapter of this thesis is aimed at summarizing all widely known solutions of extracting excess pressure energy from water pipelines, that is Pump as turbine, axial in-line turbine, counter rotating turbine and the spherical lift turbine. Advantages and disadvantages of each solution are discussed. The conclusion is that the Pump as turbine is currently the most widely used method mainly for its economic viability, its biggest drawback is the lack of regulation and the need of civil work to the site. The axial inline turbine is technically the most simple solution, main advantage is the possibility of inline installation, the turbine is currently being distributed by several companies specifically for PRV harvesting. The counter rotating turbine is a fairly new concept, it has the advantage of the axial turbine, the inline installation but also with a larger available operating conditions and better regulation capabilities. Technically this is the most elegant solution, its drawback being technical complexity and cost. But with wide enough use the price would trickle down, this could potentially make it the most effective solution.

The second chapter is dedicated to designing an axial turbine to a specific location in Austria. The design started with the determination of blade angles at the inlet and outlet, camber line was afterwards created. Thickness distribution of NACA 0012 was then applied. The biggest shortcoming in the first iteration was low utilized head, only 18.6 %, efficiency recorded was 77 %. This was corrected in the second iteration by adding more blades, 77 % of utilized head was achieved with slightly lower efficiency of 68 %. In further iterations it would be suggested that the angle β_2 would be increased to utilize even more energy, a different and more complex camber line function could be used for better efficiency. In the last simulation the counter rotating concept was imitated. Utilized energy was almost two times the projected one at 202 %. This shows the big operation ranges of the counter rotating turbine. To correct this a lower number of blades would be chosen with the constraint of the numbers of individual runners being incommensurable to avoid pressure pulsation of the interacting blades. Quite high efficiency of 71 % was achieved.

Literature

- [1] Cumulative renewable electricity capacity in the main and accelerated cases and Net Zero Scenario. 2021-2030. Available also from: <https://www.iea.org/data-and-statistics/charts/cumulative-renewable-electricity-capacity-in-the-main-and-accelerated-cases-and-net-zero-scenario-2021-2030>.
- [2] BEDNÁŘ, Josef. Turbíny. 2013, 00360s. Available from DOI: [ISBN978-80-905437-0-6](https://doi.org/10.1016/j.renene.2022.05.128).
- [3] PARTNER, Jaberg und. Set-up of a model experiment - pump as turbine. 2023. Available also from: <https://www.jabergundpartner.com/en/news/blog/the-pump-as-a-turbine-application-in-industrial-processes/>.
- [4] ORCHARD, Bryan. Pumps as turbines in the water industry. 2009. Available also from: <https://www.worldpumps.com/content/features/pumps-as-turbines-in-the-water-industry/>.
- [5] MARINI, Gustavo; MAIO, Marco; DI MENNA, Francesco; PUGLIESE, Francesco; DE PAOLA, Francesco; FONTANA, Nicola. Innovative Approach for Selection of Pump as Turbine in Water Distribution Network. *Environmental Sciences Proceedings*. 2022, vol. 21, no. 1. ISSN 2673-4931. Available from DOI: [10.3390/environsciproc202202102](https://doi.org/10.3390/environsciproc202202102)
- [6] LE MARRE, Maël; MANDIN, Philippe; LANOISELLÉ, Jean-Louis; ZILLIOX, Erik; RAMMAL, Farah; KIM, Myeongsu (Mike); INGUANTA, Rosalinda. Pumps as turbines regulation study through a decision-support algorithm. *Renewable Energy*. 2022, vol. 194, pp. 561–570. ISSN 0960-1481. Available from DOI: <https://doi.org/10.1016/j.renene.2022.05.128>.
- [7] *Notes from Brno University of technology, Faculty of Mechanical Engineering*. [N.d.].
- [8] MELICHAR Jan, Jan VOJTEK a Jaroslav BLÁHA. Malé vodní turbíny: konstrukce a provoz. Praha: Vydavatelství ČVUT, 1998, 299s. Available from DOI: [ISBN80-01-01808-3](https://doi.org/10.13140/RG.2.1.4523.3127).
- [9] KRAMER, Matthias; WIEPRECHT, Silke. Investigations on micro-hydro turbines in drinking water supply systems. In: 2012.
- [10] RESIGA, Romeo; MUNTEAN, Sebastian; STUPARU, Adrian; NEIPP, Andreas; RUPRECHT, A.; RIEDELBAUCH, Stefan. ON THE HUB-TO-SHROUD RATIO OF AN AXIAL EXPANSION TURBINE FOR ENERGY RECOVERY. In: 2015. Available from DOI: [10.13140/RG.2.1.4523.3127](https://doi.org/10.13140/RG.2.1.4523.3127).
- [11] BUCK. [N.d.]. Available also from: <https://www.stellba-hydro.de/en/water-turbines/axent-turbine/>.
- [12] LISZKA, Damian; BORKOWSKI, Dariusz; GRĄDZIEL, Sławomir. Integrated turbine-generators for hydropower plant – a review. *E3S Web of Conferences*. 2021, vol. 323, p. 00022. Available from DOI: [10.1051/e3sconf/202132300022](https://doi.org/10.1051/e3sconf/202132300022).
- [13] MÜNCH, Cecile; RICHARD, Sylvain; B., Meier; HASMATUCHI, Vlad; AVELLAN, François. Numerical Simulations of a Counter Rotating Micro Turbine. In: 2012.
- [14] KANEMOTO, Toshiaki; OBA, Shin. Proposition of Unique Pumping System with Counter-Rotating Mechanism. *International Journal of Rotating Machinery*. 1900, vol. 10, p. 462402. ISSN 1023-621X. Available from DOI: [10.1155/S1023621X04000259](https://doi.org/10.1155/S1023621X04000259).

- [15] HASMATUCHI, Vlad; MÜNCH, Cecile; GABATHULER, Shadya; CHEVAILLER, Samuel; AVELLAN, François. New Counter-Rotating Micro-Hydro Turbine for Drinking Water Systems. 2014.
- [16] XIULI, Wang; BIN, Lin; YANG, Li; YAN, Zhang; RONGSHENG, Zhu; YUN, Long; QIANG, Fu. Hydraulic Optimization of Two-Way Counter-rotating Axial Flow Pump Turbine. *Frontiers in Energy Research*. 2020, vol. 8. ISSN 2296-598X. Available from DOI: [10.3389/fenrg.2020.577232](https://doi.org/10.3389/fenrg.2020.577232).
- [17] CASINI, Marco. Harvesting energy from in-pipe hydro systems at urban and building scale. *International Journal of Smart Grid and Clean Energy*. 2015, vol. 4. Available from DOI: [10.12720/sgce.4.4.316-327](https://doi.org/10.12720/sgce.4.4.316-327).
- [18] GHADA DIAB, Mohamed Elhakeem; SATTAR, Ahmed M.A. Performance assessment of lift-based turbine for small-scale power generation in water pipelines using OpenFOAM. *Engineering Applications of Computational Fluid Mechanics*. 2022, vol. 16, no. 1, pp. 536–550. Available from DOI: [10.1080/19942060.2021.2019129](https://doi.org/10.1080/19942060.2021.2019129).
- [19] FLEISCHNER P., Nechleba M. Hydromechanika hydraulických strojů, Skripta VUT v Brně. 1976. Available from DOI: [ISBN80-214-0226-1](https://doi.org/10.1080/19942060.2021.2019129).
- [20] CELIK, Yunus. A Comparative Aerodynamic Analysis of NACA and NREL Aerofoils for Darrieus Turbines Using CFD. 2022. Available from DOI: [10.46460/ijiea.1075684](https://doi.org/10.46460/ijiea.1075684).
- [21] [N.d.]. Available also from: <http://airfoiltools.com/airfoil/naca4digit>.
- [22] JOUSEFM. [N.d.]. Available also from: <https://www.simscale.com/forum/t/what-is-y-yplus/82394>.

NOMENCLATURE

Abbreviations	Meaning
PAT	Pump as turbine
BEP	Best efficiency point
CFD	Computational fluid dynamics
PRV	Pressure reduction valve
AXENT	Axial expansion turbine
STRAFLO	Straight flow turbine
NACA	National Advisory Committee for Aeronautics
TSR	Tip speed ratio
SST	Shear stress transport
CAD	Computer aid design

Acronym	Unit	Description
E	[J/kg]	Specific energy
m	[kg]	Mass
E_z	[J/kg]	Potential specific energy
E_k	[J/kg]	Potential kinetic energy
E_p	[J/kg]	Potential pressure energy
P	[J/s]	Power
ρ	[kg/m ³]	Density
Q	[m ³ /s]	Flow rate
η	[1]	Efficiency
P_{flow}	[J/kg]	Theoretical power of the flow
P_t	[J/kg]	Power on the shaft
\vec{c}	[m/s]	Absolute velocity
\vec{u}	[m/s]	Translational velocity
\vec{w}	[J/kg]	Relative velocity
c_u	[m/s]	Absolute velocity component in the translational direction
M_k	[Nm]	Torque
ω	[rad/s]	Angular velocity
σ	[1]	Rotor solidity
D	[m]	Diameter
TSR	[1]	Tip speed ratio
U	[m/s]	Free stream velocity
g	[m/s ²]	Gravitational acceleration
H	[m]	Head
S	[m ²]	Cross sectional area
β_1	[rad]	Blade angle at the inlet
β_2	[rad]	Blade angle at the outlet
y_T	[1]	Half of blade thickness
T	[1]	Blade thickness constant
y_+	[1]	yplus parameter
μ	[Pa/s]	Dynamic viscosity
τ_ω	[Pa]	Wall shear stress
ν	[m ² /s]	Kinematic viscosity
u_t	[m/s]	Friction velocity
y	[m]	Absolute distance from the wall
τ	[Pa]	Shear stress
z	[1]	Number of blades